VECTOR CONTROL OF FOUR SWITCH THREE PHASE INVERTER FED INTERIOR PERMANENT MAGNET SYNCHRONOUS MOTOR DRIVE WITHOUT POSITION SENSOR

Kalyan Kumar HALDER
Department of Electrical & Electronic Engineering, Khulna University of Engineering & Technology, Bangladesh,
Phone: +880-1710752236, E-mail: kalyan_kuet@yahoo.com

Bashudeb Chandra GHOSH
Department of Electrical & Electronic Engineering, Khulna University of Engineering & Technology Bangladesh,
Phone: +880-1711190490, E-mail: bcgkuet@gmail.com

Abstract: *This paper proposes a vector control methodology for Four Switch Three Phase (FSTP) inverter fed Interior Permanent Magnet Synchronous Motor (IPMSM) drive with Real Time Recurrent Neural Network (RTRNN) based stator flux estimator. In the proposed control scheme, instead of a usual Six Switch Three Phase (SSTP) inverter a Four Switch Three Phase (FSTP) inverter is used. This reduces the cost of the inverter, the switching losses, and the complexity of the control board for generating six Pulse Width Modulated (PWM) signals. A simulation model of the drive system is developed and used in this paper. A Proportional plus Integral (PI) controller is used to process the speed error. Closed loop vector control technique with Clarke's transformation is used in this study. Two independent hysteresis current controllers with a suitable hysteresis band are utilized for inverter switching. The robustness of the drive system is tested for different operating conditions and found to work acceptably under these conditions.*

Key words: *Four switch three phase inverter, interior permanent magnet synchronous motor, real time recurrent neural network and sensorless control.*

1. Introduction

In recent years, permanent magnet synchronous motors (PMSM) have been widely use in several areas such as traction, automobiles, robotics, and aerospace technology [1]. The power density of PMSM is higher than one of induction motor with the same ratings because no stator power is dedicated to the magnetic field production. Nowadays, PMSM is designed not only to be more powerful but also with lower mass and lower moment of inertia [2]. Hence, PMSM drives are a topic of interest of the current researchers and different control schemes are being developed for speed control purposes.

With the invention of high speed power semiconductor devices six switch three phase inverters become popular for variable speed ac drives. But these inverters have some disadvantages such as losses in the six switches, complexity of the control algorithms and generating six PWM logic signals [3-6]. Many researchers have been working in this area to reduce the inverter size and cost without altering the drive performances. In [3] an AC to AC converter is developed for three phase Induction Motor (IM) with minimum hardware and improved power factor. A cost effective FSTP inverter is proposed for IM drive in [4]. The authors also show a performance comparison of the FSTP inverter fed drive with SSTP inverter fed drive in terms of speed response and total harmonic distortion of the stator current. The same authors propose fuzzy logic controller (FLC) based control scheme for FSTP fed IPMSM drive [5]. An entire implementation for vector control of induction motor using FSTP inverter for high performance industrial drive systems is presented in [6]. The complete vector control scheme is verified by simulation and experimentally in a DSP environment.

The rotor position information is necessary to achieve the vector control drive system of PMSM which can be detected by shaft encoder or resolver sensor. In cost sensitive applications like appliance drives or in a hostile environment, a mechanical shaft encoder can often not be used [7-8]. However, position sensors make the total system larger in volume, and less reliable. In [7] a mathematical model of IPMSM using the extended electromotive force in the rotating reference frame is utilized to estimate the rotor speed and position. A completely encoder-less Interior Permanent Magnet (IPM) motor drive with direct torque controller (DTC) is proposed in [8]. The authors use a new sliding mode observer for speed estimation. IPM motors possess magnetic saliency that introduces harmonics in the motor current. This phenomenon can be utilized to find out the rotor speed and position of the IPM drives [9]. A position sensorless control scheme for FSTP fed Brushless DC (BLDC) motor drive using a Field Programmable Gate Array (FPGA) is presented in [10].

This paper investigates the performances of position sensorless interior permanent magnet synchronous motor drive fed from four switch three phase inverter. The absence of position sensor and reduced inverter size make the drive system more attractive for industry applications. A mathematical model of IPMSM using the stator flux estimator is utilized to estimate the rotor position. A real time recurrent neural network based adaptive integration methodology is proposed for stator flux estimation to

improve the transient and steady-state performances. Estimated flux components are obtained from speed error and α- and β-axis stator current components. Moreover, the hysteresis controller is used to control the current so that it can follow the command current as close as possible to the sinusoidal reference. The performances of the proposed drive have also been studied for sudden change of load torque, parameter variations, and speed reversal conditions.

2. Mathematical Model of IPMSM

A mathematical model of the IPMSM is required for proper simulation of the system. Fig. 1 shows the different axes of IPMSM. The dynamic model of the IPMSM motor in the synchronously rotating d-q reference frame can be expressed as follows [11]:

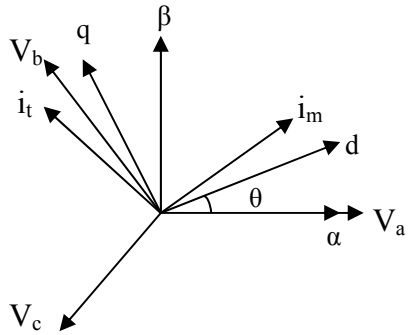

Fig. 1 Stationary and rotating axes of IPMSM

$$v_d = Ri_d + pL_d i_d - \omega_r L_q i_q \quad (1)$$

$$v_q = Ri_q + pL_q i_q + \omega_r \psi_f + \omega_r L_d i_d \quad (2)$$

$$\lambda_q = L_q i_q \quad (3)$$

$$\lambda_d = L_d i_d + \psi_f \quad (4)$$

The developed electromagnetic torque is given as:

$$T_e = \frac{3P_p}{2}(\psi_f i_q + (L_d - L_q) i_d i_q) \quad (5)$$

The mechanical motion of the IPMSM can be expressed as:

$$T_e = T_L + J_m p\omega_m + B_m \omega_m \quad (6)$$

$$\omega_r = p_p \cdot \omega_m \quad (7)$$

Where,

v_d and v_q = the dq- axis stator voltages;
i_d and i_q = the dq- axis stator currents;
λ_d and λ_q = the dq- axis stator flux linkages;
L_d and L_q = the dq- axis inductances;
ψ_f = the permanent magnetic flux linkage;
R = the stator resistance;
ω_r = the angular speed of rotor;
ω_m = the mechanical speed of rotor;
T_e = the electromagnetic torque;
J_m = the motor inertia;
B_m = the motor friction coefficient;
P_p = the number of pole pairs;
$p \equiv \frac{d}{dt}$.

3. Four Switch Three Phase Inverter Model

In the four switch inverter, as shown in Fig. 2, a three phase system is obtained by connecting the phase 'c' terminal of the stator windings directly to the centre tap of the DC link capacitors. The single phase AC supply is rectified by the front-end rectifier. The capacitors are used to level the output DC voltage. The three phase voltages of the IPMSM motor can be expressed as follows [4]:

$$V_a = \frac{V_{dc}}{3}[4S_a - 2S_b - 1] \quad (8)$$

$$V_b = \frac{V_{dc}}{3}[4S_b - 2S_a - 1] \quad (9)$$

$$V_c = \frac{2V_{dc}}{3}[-S_a - S_b + 1] \quad (10)$$

Where, V_{dc} is the maximum voltage across the DC link capacitors; S_a and S_b are the switching logic (either '0' or '1').

If S_a =1 then T_1 is on and T_2 is off
If S_a =0 then T_1 is off and T_2 is on
If S_b =1 then T_3 is on and T_4 is off
If S_b =0 then T_3 is off and T_2 is on

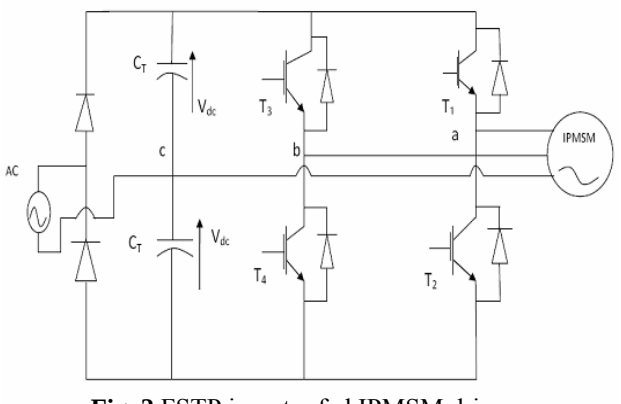

Fig. 2 FSTP inverter fed IPMSM drive.

4. Proposed Control Scheme

The proposed vector control scheme is shown in Fig. 3. The speed error is processed through a PI controller to generate the torque producing component of the stator current (i_t^*). The magnetizing component of the stator currents i_m^* along with i_t^* are then used to generate the reference currents i_a^* and i_b^*. Two independent hysteresis current controller with a suitable hysteresis band are used to command the motor currents i_a, and i_b to follow the reference currents. The hysteresis controllers also generate four switching signals which will fire the power

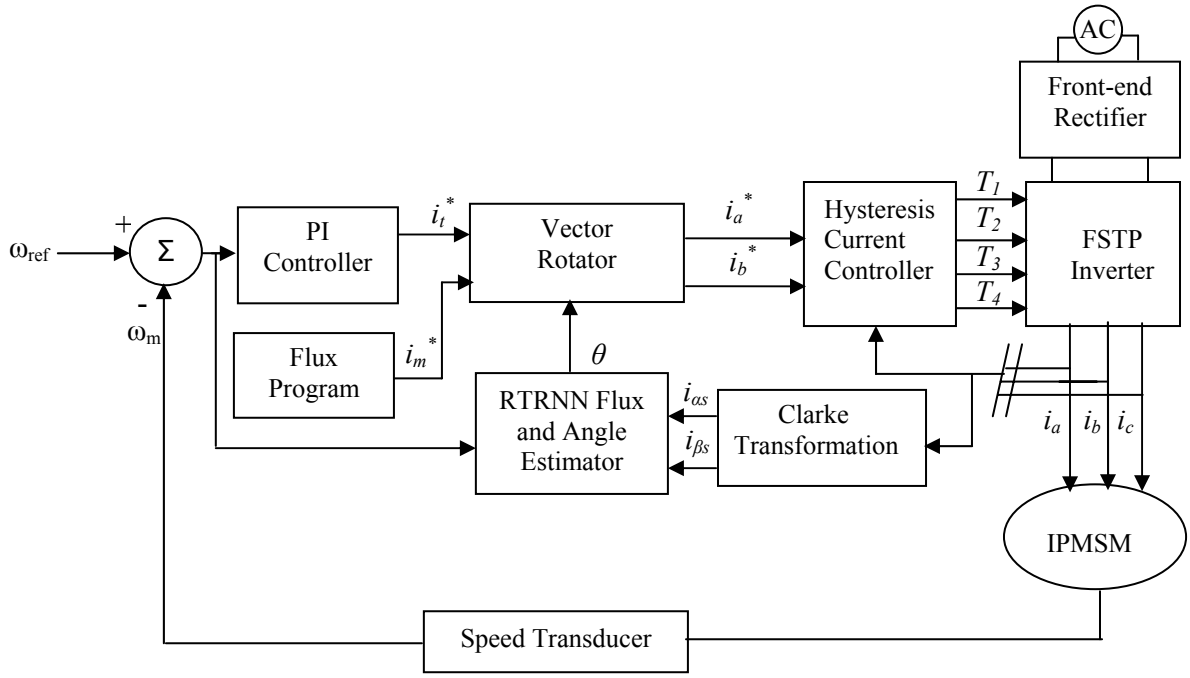

Fig. 3 Proposed Control Scheme of the IPMSM.

semiconductor devices of the three phase inverter to Produce the actual voltages to the motor. The three phase motor currents i_a, i_b, and i_c are transformed into α-, and β-axis components through Clarke transformation.

The Real Time Recurrent Neural Network (RTRNN) is a single layer neural network with input and output nodes. The output nodes act as summing nodes and in this study the two output variables, i.e., α- and β-components of stator flux linkage are fed to the input with unit delay operator. The value of activation function at the output node is taken unity. The common inputs for both the outputs are α- and β-components of stator current and the speed error which results in the following matrix equation [12]:

$$\begin{bmatrix}\lambda_{\alpha s}(k+1)\\ \lambda_{\beta s}(k+1)\end{bmatrix}=\begin{bmatrix}W_{11p} & 0\\ 0 & W_{22p}\end{bmatrix}\begin{bmatrix}\lambda_{\alpha s}(k)\\ \lambda_{\beta s}(k)\end{bmatrix}+\begin{bmatrix}W_{11}\\ W_{21}\end{bmatrix}i_{\alpha s}(k)$$
$$+\begin{bmatrix}W_{12}\\ W_{22}\end{bmatrix}i_{\beta s}(k)+\begin{bmatrix}W_{13}\\ W_{23}\end{bmatrix}E_{\omega}(k) \quad (11)$$

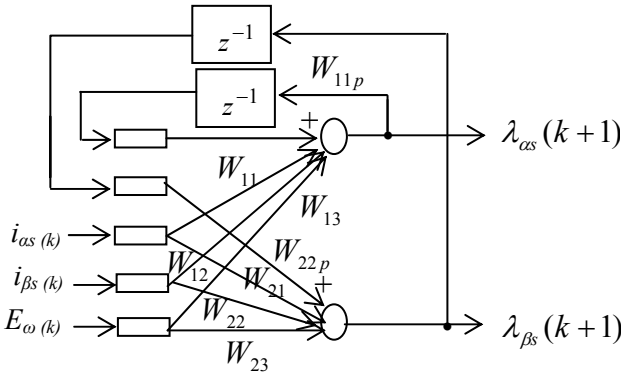

Fig. 4 Stationary α- and β- axis stator flux estimation by RTRNN.

The inputs are connected to the output node through the weights W_{11}, W_{12}, W_{21}, W_{22} etc. as indicated by the line segments and shown in Fig. 4. Each output node is also connected to the corresponding recurrent input node through weights. The weights indicated by the different line segments are adjusted by training the neural network.

Estimated angle of reference pole,

$$\theta=\tan^{-1}\left(\frac{\lambda_{\beta s}}{\lambda_{\alpha s}}\right) \quad (12)$$

The reference currents are formulated as follows:

$$i_a^*=i_m^*\cos\theta-I_t^*\sin\theta \quad (13)$$

$$i_b^*=i_m^*\cos(\theta-120^0)-I_t^*\sin(\theta-120^0) \quad (14)$$

The stationary 3-axes (a-, b-, c-) to stationary 2-axes (α-, β-) transformation is given by

$$i_{\alpha s}=i_a-0.5\,i_b-0.5\,i_c \quad (15)$$

$$i_{\beta s}=\frac{\sqrt{3}}{2}(i_b-i_c) \quad (16)$$

5. Simulation Results

Computer simulations have been carried out in order to validate the effectiveness of the proposed control scheme under different operating conditions. The system under consideration has been simulated in the C++ environment. The name plate rating and motor parameters used in this simulation are given in Appendix.

5.1 Stator Flux and Rotor Position Estimation

The performance of the proposed RTRNN has been

demonstrated before implementing it in the drive system. Fig. 5 (a) & (b) show the actual and estimated responses of α- and β-axis stator flux components under transient condition. Fig. 5 (c) shows the actual and estimated rotor angle under transient condition. Similarly, Fig. 6 (a) & (b) show the actual and estimated responses of α- and β-axis stator flux components under steady-state condition.

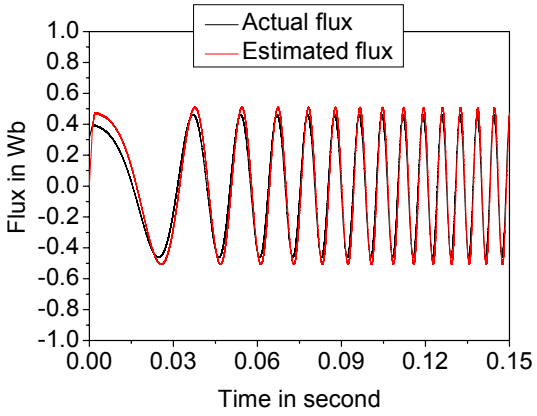

(a)

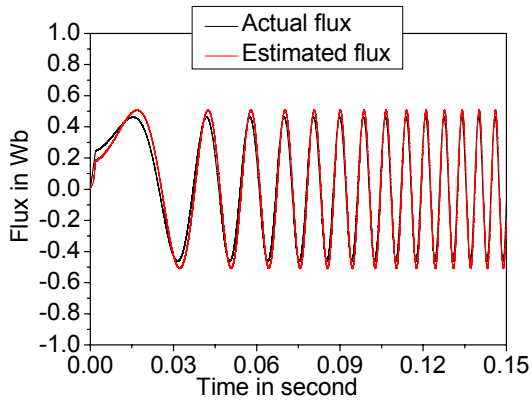

(b)

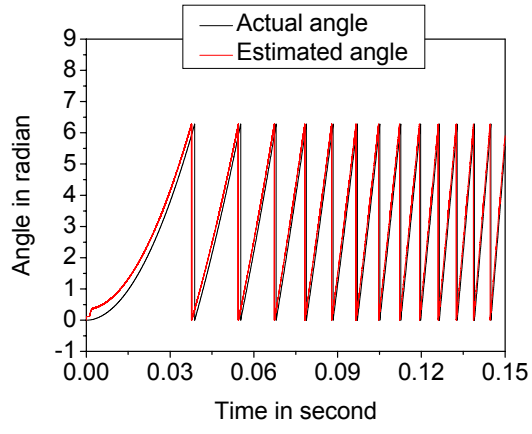

(c)

Fig. 5 Actual and estimated responses of (a) α-axis stator flux, (b) β-axis stator flux, and (c) Rotor angle for the IPMSM drive under transient condition.

Fig. 6 (c) shows the actual and estimated rotor angle under steady-state condition. From the figures it is apparent that the estimated responses are matching absolutely with the actual responses both in transient and steady-state conditions. Thus the acceptability of the proposed RTRNN has been confirmed.

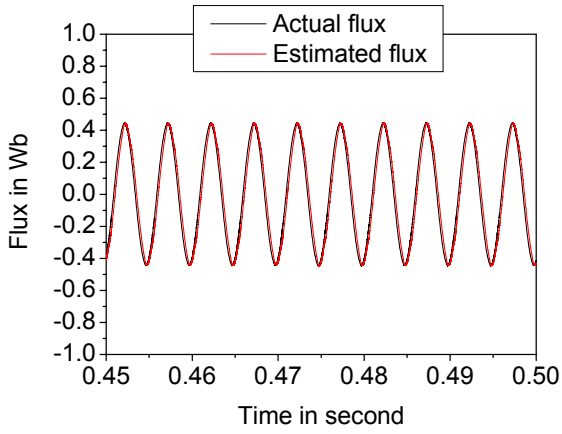

(a)

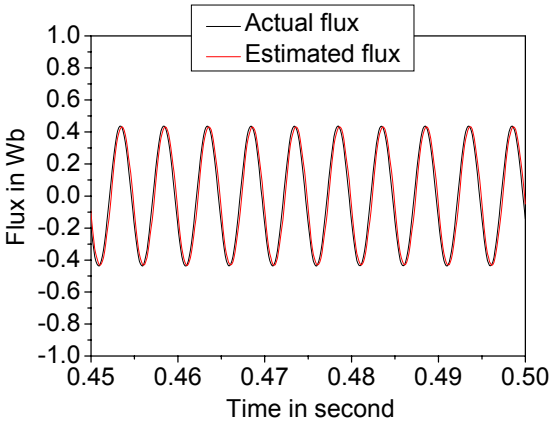

(b)

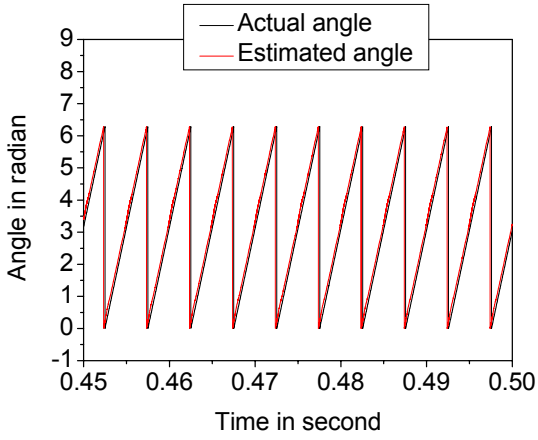

(c)

Fig. 6 Actual and estimated responses of (a) α-axis stator flux, (b) β-axis stator flux, and (c) Rotor angle for the IPMSM drive under steady-state condition.

5.2 Starting Performance of the IPMSM Drive

The motor was started with a command speed of 1500 rpm and load torque of 1.0 N-m from standstill condition. At t=0.45 second the motor reaches to the command speed. Fig 7 (a) shows the speed response of the IPMSM drive. The actual speed follows the command speed accurately without steady-state error and oscillations. Fig. 7 (b) shows the developed electromagnetic torque of the drive under starting condition. It is observed that higher electromagnetic torque is generated during the motor acceleration. Some oscillations in electromagnetic torque is noticed which is due to switching of the devices with hysteresis controller. Difference between developed and load torques is due to viscous damping torque of the drive system. Fig. 8 (a) and (b) show the actual phase currents under transient and steady-state condition.

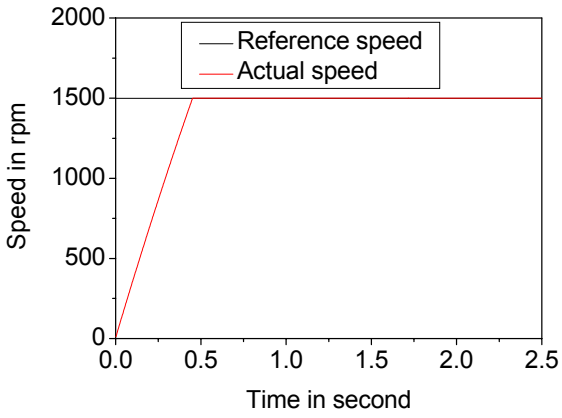

(a)

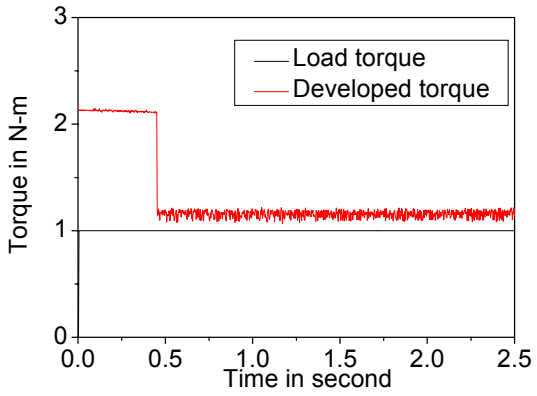

(b)

Fig. 7 (a) Simulated speed response, and (b) Developed electromagnetic torque for the IPMSM drive under transient and steady-state condition.

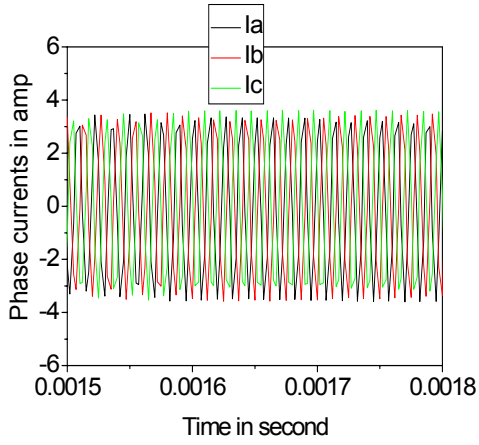

(a)

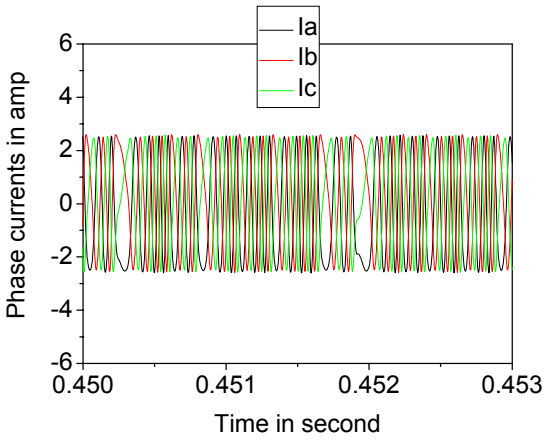

(b)

Fig. 8 Three phase actual currents under (a) Transient condition, and (b) Steady-state condition for the IPMSM drive.

5.3 Performance under Different Operating Conditions

The performance of the IPMSM drive under different operating conditions was also investigated in order to verify the robustness of the proposed control scheme. The load torque of the motor was suddenly increased from 1.0 N-m to 2.0 N-m at t=1.0 second when the motor has started from stalled condition at t=0.0 second. The developed electromagnetic torque and speed response with change of load is given in Figs. 9 (a) and (b) respectively. No fall and oscillation in speed is noticed due to this load torque disturbance. This indicates the robustness of the drive system.

To observe the effect of parameter variations, the motor stator resistance was doubled (keeping other parameters constant) at t=1.0 second. Fig. 10(a) shows

the effect of stator resistance change on speed response. The speed does not drop at all due to change of stator resistance. The stator inductances (d- and q-axis) was increased to double (keeping other parameters constant) at t=1.0 second. Fig. 10 (b) shows the effect of inductances on speed response. The speed does not drop or rise due to change of q-axis and d-axis inductances. Thus the drive performance is insensitive of stator parameter variations.

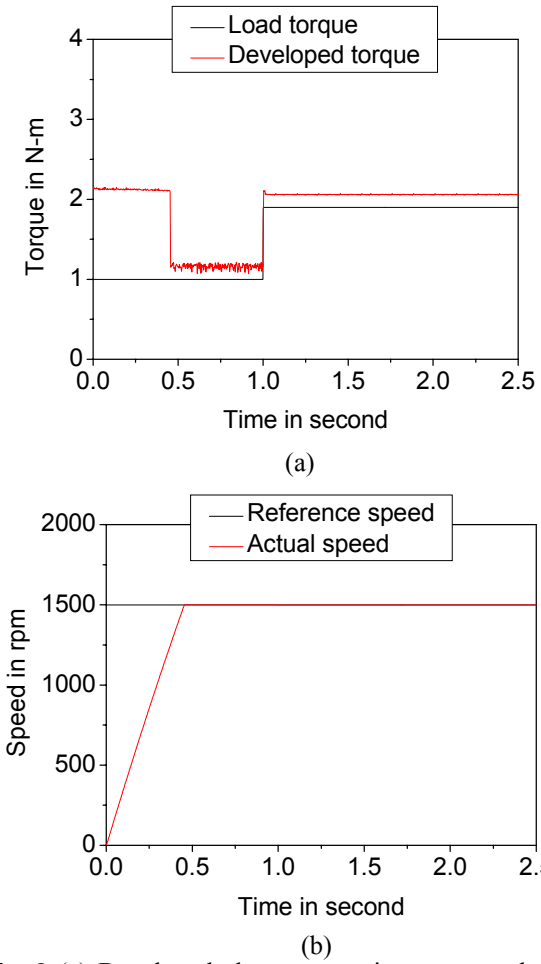

Fig. 9 (a) Developed electromagnetic torque, and (b) Simulated speed response for the IPMSM drive for change of load torque (1.0 N-m to 2.0 N-m).

To monitor the effect of speed reversal, the command speed was reversed from 1500 rpm to -1500 rpm at t=0.6 second and again to 1500 rpm at t=1.4 second. Fig. 11 (a) shows the speed response for different set of speed. It is observed that the drive system follows a linear pattern and takes smaller time to reach from 1500 rpm to -1500 rpm in comparison to starting condition (0 to +1500 rpm). Fig. 11 (b) shows corresponding developed electromagnetic torque of the IPMSM drive.

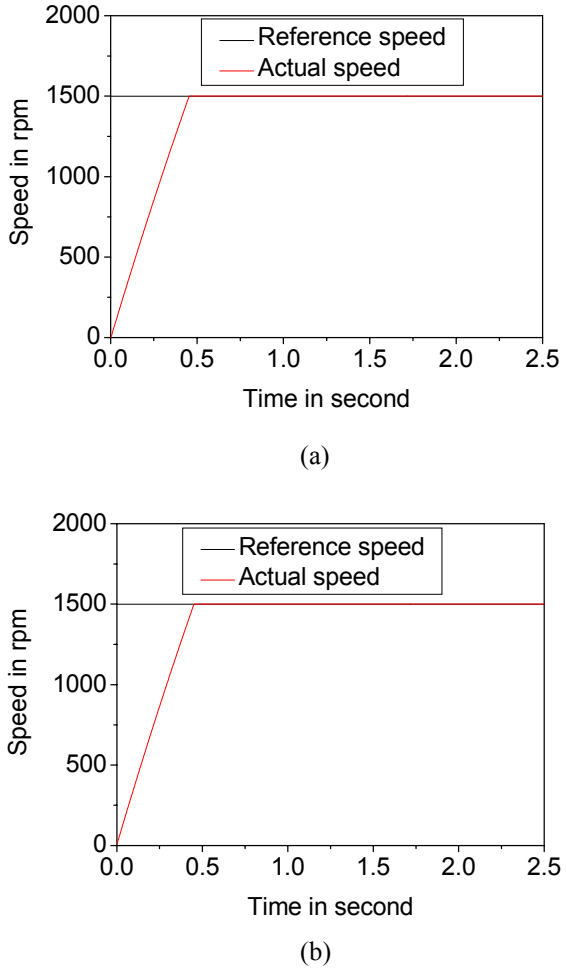

Fig. 10 Simulated speed response for (a) Change of stator resistance (R to 2R), and (b) Change of stator inductances (L_d to $2L_d$ and L_q to $2L_q$) for the IPMSM drive.

6. Conclusions

This paper presents a position sensorless control methodology for four switch three phase inverter fed interior permanent magnet synchronous motor drive. The results obtained and presented in this work indicate that the proposed control scheme produces very fast response of the IPMSM drive. It is also observed that the proposed drive with RTRNN based flux estimator is capable to estimate stator flux and rotor position both in steady-state and transient conditions accurately. The drive is also robust to load disturbances, parameter variations, and speed reversal conditions. The proposed control scheme with low cost fulfills all the necessary requirements needed for industry applications.

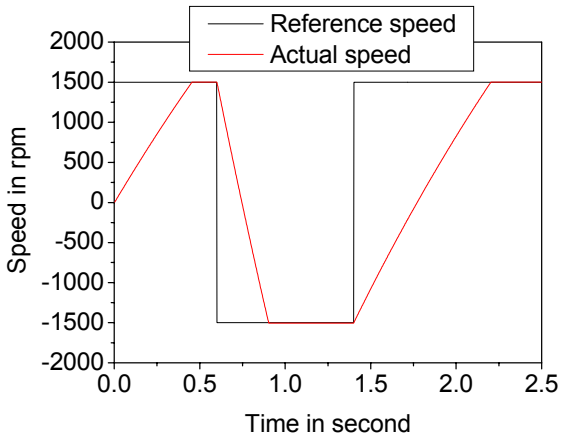

(a)

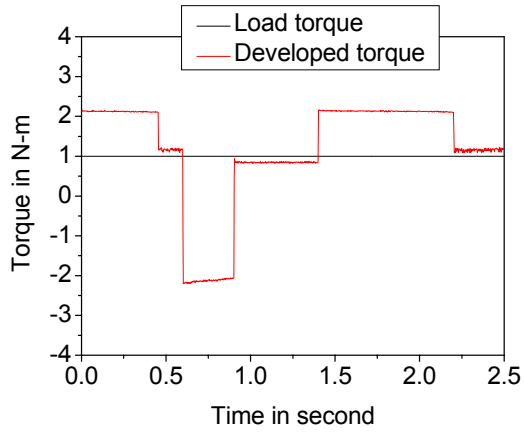

(b)

Fig. 11 (a) Simulated speed response, and (b) Developed electromagnetic torque for the IPMSM drive for change of command speed from 1500 rpm to -1500 rpm and again to 1500 rpm.

Appendix

The motor parameters are summarized below:
Interior permanent magnet synchronous motor,
Rating: 3-phase, 1 hp, 208 V, 3A, 2-pole pair.
Parameters:

Stator resistance, $R = 1.3\ \Omega$
d-axis inductance, $L_d = 0.04244$ H
q-axis inductance, $L_q = 0.07957$ H
Motor inertia, $J_m = 0.003$ Kg-m^2
Friction coefficient, $B_m = 0.001$ N-m/rad/sec
Magnetic flux constant, ψ_f (rms) = 0.311 Volts/rad/sec

References

1. Dehkordi A. B., Gole A. M., Maguire T. L.: *Permanent Magnet Synchronous Machine Model for Real-Time Simulation*. In: Proceedings of the International Conference on Power Systems Transients IPST'05, June 19-23, 2005, Montreal, Canada, paper no. IPST05-159.
2. Kaewjinda, WEERA, Konghirun, MONGKOL: *Vector Control Drive of Permanent Magnet Synchronous Motor Using Resolver Sensor*. In: ECTI Transactions on Electrical Eng., Electronics, and Communications, V(2007), No.1, February 2007, p.134-138, Thailand
3. Saravanasundaram, S., Thanushkodi, K.:*Compound Active Clamping Boost Converter-Three Phase Four Switch Inverter Fed Induction Motor*. In: International Journal of Computer Science and Network Security, VIII (2008), No. 8, August 2008, p. 358-361, Korea.
4. Uddin, M. N., Radwan, T. S., Rahman, M. A.: *Performance Analysis of a Cost Effective 4-Switch, 3-Phase Inverter Fed IM Drive*. In: Iranian Journal of Electrical and Computer Engineering, V (2006), No.2, Summer-Fall 2006, p. 97-102, Iran.
5. Uddin, M. N., Radwan, T. S., Rahman, M. A.: *Fuzzy-logic-controller-based cost effective four-switch three-phase inverter-fed IPM synchronous motor drive system*. In: IEEE Trans. on Industry Applications, XLII (2006), No.1, January /February 2006, p. 21-30, USA.
6. Dzung PHAN QUOC, Phuong LE MINH , Binh TRAN CONG, Hoang NGUYEN MINH: *A Complete Implementation of Vector Control for a Four-Switch Three-Phase Inverter Fed IM Drive*. In: Proceedings of the International Symposium on Electrical & Electronics Engineering, October 24-25, 2007, HCM City, Vietnam, p. 297-301.
7. Tanaka, KOJI, Miki, ICHIRO: *Position Sensorless Control of Interior Permanent Magnet Synchronous Motor Using Extended Electromotive Force*. In: Electrical Engineering in Japan, CLXI (2007), No.3, July 2007, p. 41-48, Japan.
8. Xu Z., Rahman M. F.: *Encoder-Less Operation of a Direct Torque Controlled IPM Motor Drive with a Novel Sliding Mode Observer*. In: Proceedings of the Australasian Universities Power Engineering Conference AUPEC 2004, September 26-29, 2004, Brisbane, Australia, paper ID 113.
9. Ogasawara, SATOSHI, Akagi, HIROFUMI: *Implementation and Position Control Performance of a Position-Sensorless IPM Motor Drive System based on Magnetic Saliency*. In: IEEE Trans. on Industry applications, XXXIV (1998), No.4, July/ August, 1998 p. 806-812, USA.
10. Lin, CHENG-TSUNG, Hung, CHUNG-WEN, Liu, CHIH-WEN: *Position Sensorless Control for Four-Switch Three-Phase Brushless DC Motor Drives*. In: IEEE Transactions on Power Electronics, XXIII (2008), No.1, January, 2008, p. 438-444, USA.

11. Ohm D.Y., Brown J.W., Chava V.B.: *Modeling and Parameter Characterization of Permanent Magnet Synchronous Motors*. In: Proceedings of the 24th Annual Symposium of Incremental Motion Control Systems and Devices, 5-8 June, 1995, San Jose, p. 81-86.

12. Abdur Rafiq, Md., Golam Sarwer, Mohammed, Ghosh, B.C.: *Fast Speed Response Field-Orientation Control of Induction Motor Drive with Adaptive Neural Integrator*. In: Istanbul University-Journal of Electrical & Electronics Engineering, VI (2006), No.2, 2006, p. 229-235, Turkey.